

involves interaction between the  $sp_2$  orbital on nitrogen containing the lone pair of electrons and the metal 5s, 5p, and 4d orbitals of the correct symmetry. It is significant that the energy of the lone pair orbital is not much lower than that of the  $\pi$  orbital in HCN. There is the possibility of some back-donation of electrons from the metal d orbitals to the  $\pi^*$  orbital but the overlap will be poor. The large value of  $A_N$  for this complex could arise partly from this back-donation directly to the nitrogen but could also be due to the lone pair orbital having a significant s character.  $\pi$ -s,p,d orbital overlap will be better in the end-on bonded complex than for the side-on bonded complex but  $\pi^*$ -d orbital overlap will be less. The smaller value of  $\rho_M$  for the end-on bonded complex is also indicative of stronger bonding. Annealing experiments did not, however, indicate a marked difference in stability.

Alesbury and Symons<sup>13</sup> have assigned two of the spectra produced by  $\gamma$ -irradiated frozen solutions of  $AgClO_4$  in  $CD_3CN$  and  $D_2O$  to the neutral complexes  $Ag(CH_3CN)_4$  and  $(D_2O)_nAg(CH_3CN)$ .  $Ag(CH_3CN)_4$  has the parameters  $a_{109} = -532$  G,  $A_N = 6$  G, and  $g = 1.997$ . This four ligand complex has, therefore, a  $\rho_{5s}$  which falls between the values for our two complexes whereas  $A_N$  is much smaller than our value for  $Ag[HCN]$  (species B). The value of  $\rho_{5s}$  for  $(D_2O)_nAg(CH_3CN)$  is much closer to 1 than the value of this parameter for either of our complexes.

(13) Alesbury, C. K.; Symons, M. C. R. *J. Chem. Soc., Faraday Trans. 1* 1980, 76, 244-255.

The absence of a Cu analogue to the end-on  $Ag[HCN]$  complex is perhaps surprising but is probably due to insufficient compensation by overlap with the  $\pi^*$  orbital to balance the increase in d- $\pi$  separation; such back-donation is probably the reason for the stability of the side-on copper complex. The absence of  $Au[HCN]$  complexes must be associated with the relative stabilities of the complexes and the organogold iminyl  $AuCH=N$ .

Unlike all the other group 1B complexes studied which have g factors equal to or below the free spin value the g factors for  $Cu[HCN]$  are above 2.0023. This difference is outside our experimental error and is indicative of a larger contribution to the SOMO by an underlying filled d orbital on the copper. This in itself is the result of the closer proximity of the s and d orbital energy levels for this coinage metal.

In conclusion it appears that we have observed two of the intermediates, the metal ligand complex and the metal iminyl radical,<sup>3</sup> involved in the reaction between group 1B metal atoms and hydrogen cyanide to produce ultimately the metal cyanide and hydrogen, i.e., we have established some of the elementary steps in this complex reaction mechanism.

*Acknowledgment.* We thank Dr. J. S. Tse for many helpful discussions and J.A.H. and B.M. thank NATO for a collaborative research grant.

*Registry No.* <sup>63</sup>Cu, 14191-84-5; <sup>107</sup>Ag, 14378-37-1; HCN, 74-90-8;  $CuCH=N$ , 88230-19-7;  $AgCH=N$ , 88230-20-0;  $Cu[HCN]$ , 88230-18-6;  $Ag[HCN]$  isomer I, 91760-24-6;  $Ag[HCN]$  isomer II, 91760-25-7.

## Pressure Dependence of the Laser-Initiated Isomerization of Methyl Isocyanide

M. J. Shultz,\* Elizabeth J. Rock,<sup>†</sup> Robert E. Tricca, and Loretta M. Yam

Chemistry Department, Tufts University, Medford, Massachusetts 02155 (Received: January 23, 1984; In Final Form: May 7, 1984)

The infrared laser-induced isomerization of methyl isocyanide has been investigated and found to exhibit a marked pressure dependence; i.e., for a given set of conditions, there exists a sharp threshold pressure above which there is massive isomerization. In the subthreshold region, it has been determined that the yield depends exponentially on the pressure for a multimode beam. Since other authors have suggested that this laser-induced reaction is a thermal explosion, we have also carried out a numerical simulation of this system as a thermal explosion. Both the experimental and theoretical results are presented, and the results show that the thermal explosion model does not fit the experimental data.

Since the discovery of infrared laser-initiated reactions in the early 1970s,<sup>1,2</sup> inter- and intramolecular energy transfer have been recognized to be of fundamental importance to this field. Most experiments on infrared laser-initiated reactions have been done under static and, therefore, collisional conditions which necessarily involve both types of energy transfer. However, the molecular beam experiments of Schulz et al.<sup>3</sup> have demonstrated that reaction can occur under collisionless conditions. We thus became very interested in the marked pressure (and therefore collisional) dependence of the laser-initiated isomerization of methyl isocyanide to acetonitrile. Thermally, the isomerization is a well-characterized, unimolecular reaction.<sup>4</sup> The laser-induced reaction, however, is strongly pressure dependent, exhibiting a sharp threshold pressure above which nearly complete isomerization occurs with a single pulse. Below the threshold, the yield per pulse is much less than 1% and is an exponential function of pressure. The purpose of this paper is to report these and related experimental results along with a theoretical section which examines the applicability of a thermal explosion model (previously proposed by other authors<sup>5</sup>) to this system. It will be shown that the thermal

model does not fit the experimental results.

Briefly, the paper is set out as follows: the first section describes the experimental setup, the second gives an overview of the thermal explosion model, and the third reports the experimental results. The previously proposed thermal mechanism for this reaction is developed and extended to apply to the reported experimental conditions in the fourth section which also contains a comparison between the experimental and modeled results. Finally, the fifth section summarizes the results.

### 1. Experimental Setup

Methyl isocyanide was prepared by the dehydration of *N*-methylformamide according to the method of Casanova<sup>6</sup> with

(1) Ambartzumian, R. V.; Letokhov, V. S.; Rayabov, E. A.; Chekalin, N. V. *JETP Lett. (Engl. Transl.)* 1974, 20, 597.

(2) Lyman, J. L.; Jensen, R. J.; Rink, J.; Robinson, C. P.; Rockwood, S. D. *Appl. Phys. Lett.* 1974, 27, 273.

(3) Schulz, P. A.; Sudbo, A. S.; Krajnovich, D. J.; Kwok, H. S.; Shen, Y. R.; Lee, Y. T. *Annu. Rev. Phys. Chem.* 1979, 30, 379.

(4) Schneider, F. W.; Rabinovitch, B. S. *J. Am. Chem. Soc.* 1962, 84, 4215.

(5) Bethune, D. S.; Lankard, J. R.; Loy, M. M. T.; Ors, J.; Sorokin, P. P. *Chem. Phys. Lett.* 1978, 57, 479.

<sup>†</sup> Department of Chemistry, Wellesley College, Wellesley, MA 02181.

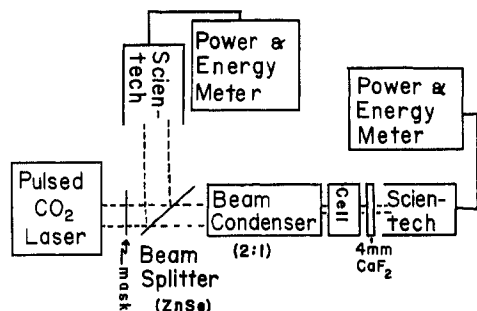


**Figure 1.** Experimental set up. For experiments with the largest diameter mask, the beam splitter was removed.

slight modification. *p*-Toluenesulfonyl chloride was recrystallized and thoroughly dried to eliminate water since hydration of the *p*-toluenesulfonyl chloride produced toluene in the isocyanide. The synthesis was initiated under an inert atmosphere of helium. The *N*-methylformamide was added over a 10-min period, and the pressure gradually reduced with a high-vacuum pump to maintain a steady distillation rate. The methyl isocyanide was collected in a trap at liquid-nitrogen temperature. To prevent the distillation of quinoline into the collection trap, a U-tube immersed in a salt-saturated, ice-water bath preceded the collection trap. Following bulb to bulb distillation, methyl isocyanide was stored in a dark vessel under vacuum. Gas chromatographic analysis revealed the product to be better than 99.5% pure.

Since methyl isocyanide absorbs into vacuum grease, it was handled in a vacuum line equipped with greaseless stopcocks fitted with Teflon O-rings. Methyl isocyanide also adsorbs rapidly onto most metals (the major exception being alloys of Ni), so the pressure was measured with a Datametrics Barocel differential manometer with an Inconel diaphragm. Cells were made of Pyrex with KCl windows attached with Duro brand plastic rubber glue. (It was determined that there was no measurable adsorption of methyl isocyanide onto the cell over a 1-h period, more than the time necessary for an experimental run.)

Samples were irradiated (see Figure 1) with a condensed (2:1) collimated beam from a grating tuned Lumonics Model 103 multimode, CO<sub>2</sub>, TEA laser. The average energy of a pulse was 3.4 J in a top-hat profile of 2.5-cm diameter when tuned to the P(34) transition of the 10.6- $\mu$ m band. Pulse energies were measured with a Scientech Model 36-0001 sensor interfaced to a Model 365 power and energy meter. After irradiation, samples were analyzed by a Hewlett-Packard Model 5750 gas chromatograph fitted with a gas injection system with a Hastalloy C rotary valve, a glass column (1/8 in.  $\times$  8 ft) packed with Chromosorb 104, and a flame ionization detector. The gas chromatograph was operated isothermally at 120  $^{\circ}$ C and interfaced to an IBM Instruments Model CS9000 microcomputer with an analog sensor board.

## 2. The Thermal Model. An Overview

Since the primary objective of this work was to determine the applicability of the previously proposed laser-induced thermal explosion model to this system, an overview of the model will be presented here, with a more detailed account of the theory in section 4. The model consists of a three-step mechanism: (1) initiation via deposition of energy by the laser followed by (2) very rapid *V-T* relaxation and adiabatic expansion and concluded by (3) competition between reaction and thermal diffusion. That is, the model assumes that the energy absorbed by the sample is quickly converted via *V-T* relaxation to thermal energy and isomerization occurs subsequent to the *V-T* relaxation according to classical thermal kinetics. Thus, the extent of isomerization is determined by the evolution of the temperature at each point in the sample.

The temperature evolution at any point and time as a result of the competition between thermal diffusion and reaction enthalpy

is given by the diffusion equation<sup>7</sup>

$$\partial\Delta T/\partial t = K\nabla^2\Delta T + \theta \quad (1)$$

where  $\Delta T$  is  $T(r,t)$  minus room temperature,  $K$  is the thermal diffusivity, and  $\theta$  is the heat source term due to the enthalpy of reaction. (The thermal diffusivity is related to the thermal conductivity,  $\kappa$  by  $K = \kappa/\rho C_p$ , where  $\rho$  is the molar density and  $C_p$  the molar heat capacity.) The heat source term,  $\theta$  is the complicating factor in this equation and is related to the specific rate constant by

$$\theta = (\Delta H/C_p)k(r,t) \quad (2)$$

where  $\Delta H$  is the molar enthalpy of reaction. Notice that the specific rate constant depends on temperature as given by the Arrhenius equation

$$k(r,t) = Ae^{-E_a/R(T_0+\Delta T)} \quad (3)$$

(where  $A$  is the preexponential factor,  $E_a$  is the activation energy, and  $T_0$  is room temperature) and hence, the heat source term also depends on temperature. It is the dependence of the heat source term on the temperature that makes this thermal diffusion equation particularly difficult. For example, if the rate of reaction is such that  $\theta$  exceeds the diffusion rate, the temperature will rise, which, in turn, increases the reaction rate, resulting in an even larger temperature rise. Conversely, if the diffusion rate is greater than  $\theta$ , then the temperature falls and the cooling rate accelerates owing to a decreased reaction rate. Only if  $\theta$  and the diffusion rate are exactly equal will the temperature remain stable. In addition, the pressures of interest are in the falloff region for this unimolecular reaction; hence, the specific rate constant also depends on the pressure. Although this pressure dependence is milder than the temperature dependence, it too must be included in eq 1 when determining both the threshold pressure and the yield. (In the simulations, the falloff effect was included as a correction factor for the specific rate constant, with the correction factor determined from the experimental rate constants of Schneider and Rabinovitch.<sup>4</sup>)

For our experimental conditions, the initial temperature profile is approximately a cylindrically symmetric, top-hat function of the radius. Qualitatively, this profile evolves as follows: the higher temperature, flat portion of the top hat rises in temperature until the diffusion front (which cools the sample) moves in from the sides of the hat and quenches the reaction. During the course of this evolution, the center of the sample attains the highest temperature. Once the cooling front has reached the center, if the temperature increase owing to reaction (i.e.  $\theta$ ) exceeds the cooling due to diffusion, the sample explodes. Conversely, if the diffusive losses exceed  $\theta$ , then the reaction is quenched. This balance determines the threshold condition for a top-hat beam profile.

The next section will refer to this qualitative discussion in presenting the experimental results, while results of the numerical simulation of the diffusion equation will be contained in section 4.

## 3. Experimental Results

The initial experiments were performed with the experimental setup shown in Figure 1 without the beam splitter or side Scientech. The mask was 2 cm in diameter, and the cell was a 2.5-cm diameter by 2.5 cm long Pyrex tube. After exiting the beam condenser, the beam was collimated (1.1-cm diameter) and had a top-hat profile. The fluence was  $2.9 \pm 0.2$  J/cm<sup>2</sup>. Under these conditions the threshold pressure is  $11.4 \pm 0.2$  torr. Above this pressure, nearly all of the material in the cell is isomerized in a single pulse even though less than one-third of the cell volume is irradiated. This almost complete isomerization has previously been observed by authors utilizing a focused beam with a Gaussian profile and attributed to a laser-initiated thermal explosion.<sup>5,8</sup>

(6) Casanova, J.; Schuster, R. E.; Werner, N. D. *J. Chem. Soc.* **1963**, 4280.

(7) Bailey, R. T.; Cruickshank, F. R.; Pugh, D.; Guthrie, F.; Johnstone, W.; Mayer, J.; Middleton, K. *J. Chem. Phys.* **1982**, *77*, 3453.

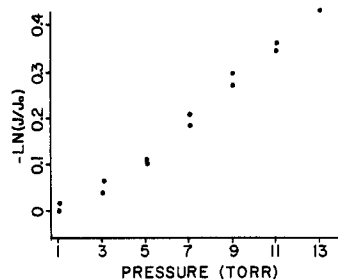


**Figure 2.** Experimental Beer's law plot. Plot of  $-\ln(J/J_0)$  vs. pressure, where  $J$  is the transmitted fluence and  $J_0$  the incident fluence. The average incident fluence was  $2.9 \text{ J/cm}^2$ , and the path length was  $40 \text{ cm}$ . From the slope, the extinction coefficient  $\xi = 9.45 \times 10^{-4} \text{ torr}^{-1} \text{ cm}^{-1}$ .

Comparison of the focused beam results with the present work indicates the value of the threshold pressure in the former is lower (this is expected since in addition to a nonuniform fluence along the cell axis, the focused beam experiments have a higher fluence at the focal point). However, except for the actual value of the threshold, our results are very similar. Isomerization is essentially complete in a single pulse and is very clean. (Analysis by gas chromatography indicates acetonitrile as the major product with a small amount of other products.)

Since the purpose of this work was to determine the limits of a thermal mechanism, three different sets of experiments were performed. (1) The energy absorbed was measured as a function of pressure for subthreshold pressure samples. The purpose of this experiment was to determine if the pressure plays a role in the excitation mechanism (e.g. bottlenecking). (2) The yield (percent converted) was determined as a function of pressure in the subthreshold region. If the threshold is a thermal explosion, then the reaction is expected to be mainly thermal at pressures near threshold (i.e. characterized by intermolecular energy transfer and modeled by the classical thermal diffusion equation). For lower pressures, the extent to which the process is thermal should fall off. (Indeed, Hartford and Tuccio<sup>8</sup> have shown that the isomerization is not thermal; i.e., they found no evidence of intermolecular energy transfer for pressures of 2 torr or less.) (3) The threshold pressure was determined for beams of different radii. As the above theoretical discussion indicates, if the threshold is determined by a thermal mechanism, then a larger radius beam should have a lower threshold because the cooling front has further to go before reaching the center of the larger beam. Hence, the central temperature rises more, resulting in a faster reaction, and diffusive losses must be greater to prevent an explosion.

As mentioned above, the motivation for the first set of experiments is to determine if the pressure plays a role in the excitation mechanism. For these experiments, the experimental setup in Figure 1 was used with a long cell (40 cm), a ZnSe beam splitter, and the side Scientech so that both  $J$  and  $J_0$  (the transmitted and incident fluence, respectively) could be determined for each pulse. If the pressure plays a role in the excitation mechanism, e.g. more efficient absorption at higher pressures (i.e. hole filling), then a deviation from the usual Beer's law type behavior should be observed as the pressure is decreased. The results are shown in Figure 2 which indicate that Beer's law is followed over the pressure range of interest (3–13 torr). Hence, increased pressure seems neither to aid nor inhibit the absorption of energy by the sample.

For the second set of experiments, the sample was irradiated with 50 pulses at less than 0.03 Hz. Since the maximum conversion is less than 7% for 50 pulses, each pulse may be considered to be independent of the previous pulses. The results of this experiment are shown in Figure 3 which indicate that the yield is an exponential function of the pressure for pressures below the threshold, while at the threshold the yield rises dramatically with reaction being nearly complete in a single pulse. A comparison of this result with those of the numerical simulation will be contained in section 4 following presentation of the simulation.

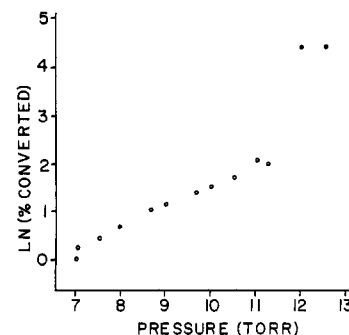


**Figure 3.** Experimental yield vs. pressure. Yield as  $\ln(\% \text{ converted})$  as a function of pressure for (O) 50 pulses and (●) 1 pulse. Note the threshold at 11.4 torr where the yield jumps from  $<0.2\%$  per pulse to greater than 85%.

**TABLE I: Experimentally Determined Explosion Pressure Threshold for Different Beam Radii**

beam radius, mm	threshold pressure, torr	$J (\pm 10\%), \text{ J/cm}^2$
5.5	12.8–13.4	2.77
4.7	12.9–13.5	2.77
3.7	13.2–13.8	2.72

This comparison will show that the model predicts a slower rise of yield with pressure than is experimentally observed.

For the third set of experiments, masks of different radii were inserted in front of the beam condenser and the threshold pressure was determined. The results in Table I indicate that, within experimental error, changing the beam radius by a factor of 1.5 while holding the fluence constant results in no change in the threshold pressure. It should be noted that since this reaction is known to be highly fluence dependent,<sup>5,9</sup> the major contribution to the uncertainty in the threshold pressure results from the uncertainty in the fluence. From the above qualitative, theoretical discussion, it is clear that if the isomerization is indeed a thermal explosion, then the threshold pressure should depend on beam radius. The numerical simulation of the thermal explosion will show that the larger beam would have a significantly lower threshold.

#### 4. The Thermal Model. A Numerical Simulation

In order to examine the above experimental results in light of a possible thermal diffusion/laser-initiated thermal explosion model, the diffusion equation analysis needs to be extended to calculate the yield in the subthreshold region and to predict the explosion threshold for a top-hat beam profile. For the three-step mechanism presented in section 2, the results of thermal lens experiments by Bailey and Cruickshank<sup>7</sup> indicate that steps 1 and 2 occur on a much faster time scale ( $\leq 50 \text{ ns}$ ) than step 3 ( $> \mu\text{s}$ ). Hence, the reaction can be modeled as evolving from an initial temperature profile determined by steps 1 and 2.

Since the absorption of laser radiation by methyl isocyanide follows Beer's law and the extinction coefficient is small (from the slope of Figure 2, the extinction coefficient,  $\xi$ , is determined to be  $9.45 \times 10^{-4} \text{ torr}^{-1} \text{ cm}^{-1}$ )

$$E_{\text{abs}} = AJ_0(1 - J/J_0) = AJ_0(1 - e^{-\xi Pl}) \approx AJ_0\xi Pl \quad (4)$$

(where  $E_{\text{abs}}$  is the energy absorbed,  $A$  is the cross-sectional area,  $P$  is the pressure, and  $l$  is the path length); i.e., the energy absorbed is approximately a linear function of pressure. Since the total heat capacity is also a linear function of pressure, the initial temperature profile ( $= E_{\text{abs}}/C_p$ ) is independent of sample pressure. Thus, the variation in the yield with pressure and the development of the explosion must be due to a changing balance between reaction and diffusion as the pressure is changed.

(9) Shultz, M. J.; Tricca, R. E., unpublished results.

(10) Benson, S. W.; Cruickshank, F. R.; Golden, D. M.; Haugen, G. R.; O'Neal, H. E.; Rodgers, A. S.; Shaw, R.; Walsh, R. *Chem. Rev.* **1969**, *69*, 279.

The next subsection will extend the thermal diffusion model to calculate the yield as a function of pressure for subthreshold samples.

**Yield.** In most kinetic experiments the temperature in the reaction vessel is carefully controlled to be constant over both time and space because the specific rate constant is a function of temperature. For a laser-induced reaction, however, this is not the case; temperature varies radially from along the beam path to the cell wall and temporally from the moment of irradiation to thermal equilibrium. Therefore, the derivation of the time dependence of the concentration must be reexamined.

For the multimode, collimated beam experiments, the beam is cylindrical. Therefore, the temperature profile (temperature as a function of  $r$ ) has cylindrical symmetry. Since the sample is a weak absorber, the variation of temperature along the cylinder axis is negligible. Hence, the specific rate constant depends only on the radius and time. From the integrated form of the rate equation, we can derive a fractional yield for each cylindrical shell from  $r$  to  $r + dr$ :

$$\text{yield}(r, r+dr) = \frac{[A]_0 - [A]_t}{[A]_0} = 1 - \exp\left\{-\int_0^t k(r, t) dt\right\} \quad (5)$$

To arrive at the total fractional yield, (5) must be integrated over  $r$ :

$$\text{yield} = \left[ \int_0^R \text{yield}(r, r+dr) r dr \right] / (R^2/2) \quad (6)$$

$$= \left\{ \int_0^R \left[ 1 - \exp\left\{-\int_0^t k(r, t) dt\right\} \right] r dr \right\} / (R^2/2) \quad (7)$$

where  $R$  is the cell radius. As outlined in section 2, the radial and time dependence of the specific rate constant is determined from a numerical solution of eq 1 for each pressure.

**Temperature Evolution.** As the above arguments indicate, for each pressure, both the time and spatial variation of the temperature must be determined in order to calculate the yield. Since the rates of thermal diffusion and reaction are slow compared to both the duration of the laser pulse and  $V$ - $T$  transfer, the initial temperature distribution is determined by the geometry of the laser beam and by the adiabatic expansion. The subsequent evolution of the temperature profile is determined by a competition between thermal diffusion and reaction enthalpy as given by eq 1.

For the present work, two different initial temperature profiles are of interest, a Gaussian profile which results from a TEM<sub>00</sub> pulse and a top-hat profile resulting from a multimode pulse. For a Gaussian profile, a stable temperature in the cell center is of special significance since the center temperature is the highest. If the central temperature rises, not only will it continue to rise, but the temperature of the region immediately adjacent to it will also rise owing to diffusion. This effect leads to a thermal explosion and isomerization of the material throughout the cell. On the other hand, if the center temperature falls, the entire temperature profile will collapse. As pointed out by Bethune et al.,<sup>5</sup> if  $\partial\Delta T/\partial t = 0$  at  $r = 0$ , then

$$\frac{2\kappa}{r_0^2 \Delta H \rho A} = \frac{e^{-E_a/R(T_0+\Delta T_i)}}{\Delta T_i} \quad (8)$$

where  $\Delta T_i$  is the initial temperature rise in the cell center. From eq 8 the explosion pressure threshold may be determined via  $\rho$  given the initial temperature rise. For subthreshold samples, the diffusion equation must be solved for the temperature profile as a function of time and space, and this profile fed into the yield (eq 7). This has been done numerically by using a Runge-Kutta method for several cases, and the evolution of a typical temperature profile is shown in Figure 4. (The values of the parameters needed for this simulation are known from previous work:  $\kappa = 6 \times 10^{-5}$  cal/(°C cm s),  $\Delta H = 14.7$  kcal/mol,  $A = 10^{13.6}$  s<sup>-1</sup>,  $E_a = 38.8$  kcal/mol (ref 4),  $C_p = 17.09$  cal/(K mol)<sup>11</sup> (ref 10), and the

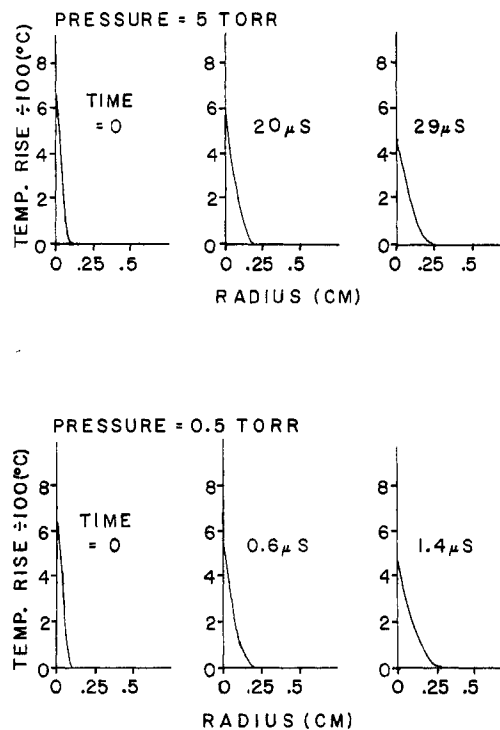


**Figure 4.** Simulated temperature profile evolution. The evolution of a Gaussian temperature profile of radius 0.033 cm with the maximum temperature rise at time zero of 630 °C for two pressures: 5.0 and 0.5 torr. Note that the 5-torr sample cools more slowly than the 0.5-torr sample.

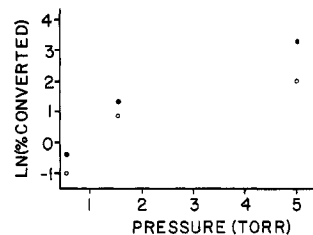


**Figure 5.** Yield vs. pressure for a Gaussian Beam. Comparison of the experimental (●) (ref 8) with the calculated (○) yield as a function of pressure for 2000 pulses with a Gaussian beam profile of radius 0.033 cm.

correction factor for the pressure dependence of the specific rate constant approximated from ref 4.). The yields computed with this method for a Gaussian profile are shown in Figure 5, along with the experimental results of Hartford and Tuccio.<sup>8</sup> Note that the experimental and calculated yields have the same qualitative behavior as a function of pressure. However, several points should be made with regard to comparison of the experimental and numerical results: First, closer agreement between the two results is not expected owing to the difficulty in determining the experimental parameters, e.g. beam radius, focal volume, and fluence. Second, the thermal model for this reaction is expected to break down at the lower pressures since Hartford and Tuccio<sup>8</sup> have shown that this reaction is isotopically selective and therefore not thermal for pressures in the 1–2-torr region. Thus, qualitative agreement in the yield data cannot be taken as proof that the reaction is thermal. In fact, the qualitative agreement between the experimental results and the numerical simulation is not surprising since it has been shown that the yield can be a very insensitive measure of the molecular energy distribution.<sup>12</sup>

Compared with the focused beam, Gaussian profile, the top-hat beam profile offers some advantages. It allows accurate determination of the experimental parameters and control over other parameters such as the beam diameter. The numerical simulation

(11) Although the heat capacity is a temperature-dependent function, for the present discussion it may be considered to be constant since the specific rate constant is highly temperature dependent. Hence, the reaction is effectively quenched within a small temperature range.

(12) Shultz, M. J.; Yablonovitch, E. *J. Chem. Phys.* **1978**, *68*, 3007.

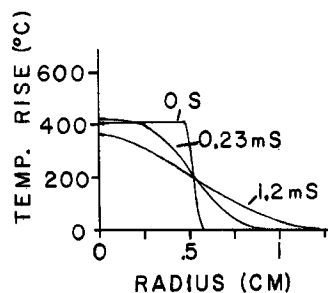


**Figure 6.** Evolution of a top-hat temperature profile. Numerical simulation of the evolution of a top-hat temperature profile of 0.5-cm radius with an initial temperature rise of 408 °C. Note that the temperature falls much more slowly than for the Gaussian profiles shown in Figure 4.

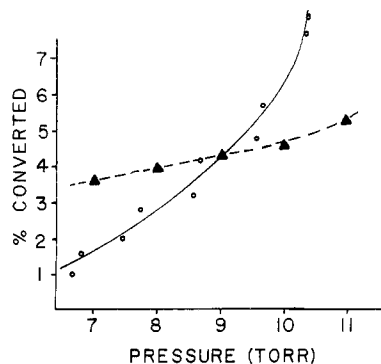


**Figure 7.** Subthreshold yield vs. pressure for a top-hat beam. Yield plotted as % converted vs. pressure in the subthreshold region for 50 pulses with a top-hat beam: (▲) modeled yields; (●) experimental results; (---) fit of the modeled results; (—) fit of the experimental results.

was therefore extended to treat a top-hat beam profile. The two most important results of the numerical simulation of the top-hat profile are, first, that the initial temperature rise needed to trigger explosion is much lower for a top-hat beam than for a Gaussian beam (e.g. for an 11.5-torr threshold, the 0.5-cm-radius top-hat beam requires a  $\Delta T_i$  of 450 °C while a Gaussian beam of 0.033-cm radius requires 590 °C). This smaller temperature rise is primarily due to the larger beam radius since the larger the radius, the longer it takes the cooling front to reach the center and quench the reaction. This is in qualitative agreement with the fact that the top-hat beam requires a lower fluence than does the focused beam to produce an explosion. The second result of the numerical simulation is that since the temperature rise for a top hat is lower, the reaction rate is smaller; thus, the rise in temperature at the center of the cell during the evolution of the temperature profile is small. (A typical evolution is shown in Figure 6.) The second result simplifies discussion of the yield as a function of pressure, while the first predicts the dependence of the explosion pressure on the beam diameter. Both of these were examined experimentally, and the results are discussed below.

The yield as a function of the pressure for subthreshold samples was modeled first, and the results are shown in Figure 7. Note that the model predicts a much slower rise with pressure than the experimental results show. Qualitatively, the numerical prediction can be understood as follows. Since the temperature rise during the evolution of the temperature profile is small, the reaction rate is essentially constant until the reaction is quenched by the cooling front. At any point  $r$ , the yield is given by eq 5. Since the product of the rate constant at the temperature of interest and the time before quenching is small ( $k \approx 1$  and the quenching time of 0.1–1 ms), the exponential can be expanded and

$$\text{yield}(r) \approx k(r) \int_0^{\text{quench time}} dt = k(r)(\text{quench time}) \quad (9)$$

Since the diffusion rate is proportional to  $1/P$ , the quench time will be roughly proportional to  $P$  and hence the yield will also be proportional to  $P$ . This is approximately what the numerical

**TABLE II: Results of the Adiabatic Expansion–Thermal Explosion Model for Various Radii<sup>a</sup>**

beam radius, mm	$r_h$	$\Delta T_i$ , °C	threshold pressure, torr
5.5	7.3	419	3.3–3.7
4.5	6.2	413	6.5–6.9
3.6	5.1	410	11.5–12
2.5	3.7	404	25.5–26

<sup>a</sup>  $r_h$  is the radius and  $\Delta T_i$  the temperature rise above room temperature for the hot zone following adiabatic expansion.

simulation shows (Figure 7). (The major deviation from linearity being due to the pressure dependence of the specific rate constant.) The experimental results show a faster rise with pressure, casting doubt on the applicability of the thermal diffusion model. (Note: As outlined in eq 5–7, the model only applies to the subthreshold region where the yield is small.)

To further test the thermal diffusion model, the dependence of the explosion on the beam size was examined. The earlier discussion of the initial temperature profile indicates that keeping the incident fluence constant is equivalent to holding the laser-induced temperature rise constant. Since the effect of adiabatic cooling is nearly the same for all irradiation volumes (see Appendix A), the initial temperature rise is approximately the same for all beam diameters which results in the cooling front reaching the center of the cell sooner for a smaller radius beam. Hence, to reach an explosion, the pressure must be higher for a smaller radius beam to slow the cooling front down; i.e., explosion will occur at a higher pressure for the same initial temperature rise but a smaller radius. The mild dependence of the specific rate constant on pressure moderates this effect somewhat; however, as the simulation results in Table II show, the modeled explosion pressure depends strongly on the radius. In fact, the results in Table II are in qualitative agreement with the analytical solution of the explosion threshold for the Gaussian beam (eq 8) which shows that  $P_{\text{exp}} \propto 1/r_0^2$ .

The experimental explosion pressure was determined as a function of beam radius, and the results are shown in Table I. A comparison of the results in Tables I and II clearly shows that experimentally the threshold is independent of the beam radius while the thermal explosion model predicts a significant rise in threshold pressure with decreasing beam radius; i.e., the model does not fit the experimental evidence.

## 5. Comments and Conclusion

Experimental results for the laser-induced isomerization of methyl isocyanide to acetonitrile have been presented and compared with the previously proposed thermal explosion model. Of the results, the existence of a pressure threshold for massive isomerization shows agreement between the experimental and the modeled results. However, neither the experimental dependence of this threshold on the beam size nor the yield as a function of pressure in the subthreshold region is in agreement with the model. Since the extent to which the process is thermal is expected to decrease as the pressure is lowered, the latter might be expected. However, the first is surprising and represents a significant failure of the thermal explosion theory to model this system.

In related work, Selamoglu and Steel<sup>13</sup> have modeled the laser-induced decomposition of cyclobutanone sensitized by hexafluorobenzene and found the thermal conductivity model in reasonable agreement with experimental results. It should be noted, however, that for sensitized experiments, (a) the reacting species is indirectly excited, (b) the energy absorbed by the sensitizer is much larger than that absorbed by methyl isocyanide, and (c) in the Selamoglu–Steel experiments, the reactant pressure was a small fraction of the total. Hence, the two experiments are not directly comparable.

Experiments currently under way in our laboratory are designed to explore the extent of intermolecular vs. intramolecular energy

transfer in the development of the massive isomerization of methyl isocyanide and will be reported in a further publication.

**Acknowledgment.** Acknowledgment for support of this work is made to the donors of The Petroleum Research Fund, administered by the American Chemical Society, to the National Science Foundation (Award No. CDP-8007856), and to the Tufts University Faculty Research Awards. M.J.S. also thanks Professor E. Grunwald for valuable assistance in the early stages of this work and Dr. E. K. Schultz (University of Minnesota) for valuable discussions concerning microcomputing equipment.

#### Appendix A

The laser-induced thermal explosion model for the isomerization of methyl isocyanide assumes that the energy absorbed from the laser beam is rapidly converted to thermal energy, resulting in a hot column of gas in the center of the cell for the top-hat geometry. This hot column then undergoes an adiabatic expansion followed by evolution of the temperature profile according to the thermal diffusion equation (eq 1). The purpose of this Appendix is to elucidate the adiabatic expansion step.

Immediately after  $V$ - $T$  relaxation, the gas in the center of the cell is hotter than the surrounding gas and hence has a higher pressure. The adiabatic expansion progresses until the pressure imbalance is relieved. This results in a volume for the hot gas,  $V_h$ , which is larger than the irradiated volume,  $V_i$ :

$$V_h = \frac{V}{\left[ \frac{V_0}{V_i} \left( \frac{P_0}{P_i} \right)^{1/\gamma} + 1 \right]} \quad (\text{A.1})$$

where  $V_0$  is the volume outside the irradiated zone,  $V$  is the cell volume, and  $P_0$  and  $P_i$  are the pressures before irradiation and immediately following  $V$ - $T$  relaxation. The adiabatic expansion also results in a slight cooling of the sample. The temperature immediately following  $V$ - $T$  relaxation ( $T_i$ ) is related to the temperature following adiabatic expansion ( $T_h$ ) by

$$\frac{T_i}{T_h} = \left[ \frac{V}{(V_0(P_0/P_i)^{1/\gamma} + V_i)} \right]^{\gamma-1} \quad (\text{A.2})$$

where  $\gamma = C_p/C_v$ . Finally, the equilibrium pressure,  $P$ , is given by

$$P = P_0 \frac{V_i T_h}{T_0 V_h} \quad (\text{A.3})$$

where  $T_0$  is room temperature.

For the beams of interest in this work, the adiabatic expansion cools the sample by about 50 °C and expands the volume from 1.3 to 1.5 times the original volume.

Registry No. Methyl isocyanide, 624-83-9.

## Search for Excitation Selectivity in Infrared Multiple Photon Dissociation. 1,1,1-Trideuterio-2,5-dithiahex-3-yne

S. Ruhman, Y. Haas,\*

Department of Physical Chemistry and The Fritz Haber Research Center for Molecular Dynamics, The Hebrew University of Jerusalem, Jerusalem 91904, Israel

J. Laukemper, M. Preuss, H. Stein, D. Feldmann, and K. H. Welge

Faculty of Physics, The University, 48D Bielefeld, Federal Republic of Germany (Received: February 14, 1984)

The question of excitation selectivity in unimolecular reactions induced by infrared multiple photon excitation (IRMPE) was probed by using the isotopically labeled molecule  $\text{CH}_3\text{SCCSCD}_3$ . The relatively rigid SCCS group was inserted in order to serve as a block to fast intramolecular energy exchange between the  $\text{CH}_3$  and  $\text{CD}_3$  moieties. Irradiation by a  $\text{CO}_2$  laser pulse could initially selectively excite either one. Probing was done in real time at low pressures ( $\sim 10^{-4}$  torr) by vacuum-UV laser single-photon ionization. At all irradiation wavelengths, equal amounts of  $\text{CH}_3$  and  $\text{CD}_3$  radicals were formed. Thus, fast intramolecular energy exchange on the time scale of the IRMPE process is directly demonstrated.

#### Introduction

Infrared multiple photon excitation (IRMPE) is now a proven and convenient method for inducing unimolecular decomposition in the gas phase under practically collision-free conditions.<sup>1</sup> The high species selectivity of this excitation method was demonstrated in isotope separation experiments.<sup>2</sup> The fundamentally more intriguing issue of mode-selective excitation has not yet been adequately addressed. Implementation of IRMPE mode-selective chemistry involves two basic requirements: a means to selectively excite a specific molecular vibrational mode, and a way to maintain the nonrandom internal energy distribution created in this way on the time scale of the decomposition process.

At present, the vast majority of IRMPE reactions have been interpreted by invoking the statistical theory of unimolecular reactions.<sup>3</sup> Chemical activation (CA) experiments<sup>4</sup> have shown that in many cases redistribution of vibrational energy in highly excited polyatomic molecules is completed in  $10^{-12}$ – $10^{-11}$  s. This process is thus much faster than the IRMPE one, which consists of successive absorption of many infrared photons. In most experiments the energy acquisition process lasts  $10^{-7}$ – $10^{-6}$  s, and in those conducted by employing short laser pulses, the typical time scale is  $10^{-9}$  s.<sup>5</sup> Moreover, the current theory of IRMPE

(1) Recent reviews are: King, D. S. *Adv. Chem. Phys.* **1982**, *50*, 105. Quack, M. *Adv. Chem. Phys.* **1982**, *50*, 395.

(2) See for example: Marling, J. B.; Herman, I. P.; Thomas, S. J. *J. Chem. Phys.* **1980**, *72*, 5603. Evans, D. K.; McAlpine, R. D.; Adams, H. M. *J. Chem. Phys.* **1982**, *77*, 3551.

(3) Robinson, P. J.; Holbrook, K. A. "Unimolecular Reactions"; Wiley-Interscience: New York, 1982. Forst, W. "Theory of Unimolecular Reactions"; Academic Press: New York, 1973.

(4) Oref, I.; Rabinovitch, B. S. *Acc. Chem. Res.* **1979**, *12*, 166. Rynbrandt, J. D.; Rabinovitch, B. S. *J. Phys. Chem.* **1971**, *75*, 2164.

(5) Kolodner, P.; Winterfeld, C.; Yablonovitch, E. *Opt. Commun.* **1977**, *20*, 119. Pasternak, A. W.; James, D. J.; Nilson, J. A.; Evans, D. K.; McAlpine, R. D.; Adams, H. M.; Selkirk, E. B. *Appl. Opt.* **1981**, *20*, 3849.